8

The Convergence Analysis of Feedforward Active Noise Control System

Guoyue Chen
Akita Prefectural University
Japan

1. Introduction

Most active noise control (ANC) systems [1-3] are based on feedforward structure with adaptive filters, which are updated with the filtered-x LMS algorithm [4, 5] or the multiple error filtered-x (MEFX) LMS algorithm [6, 7]. The convergence characteristics of these algorithms have been studied mostly in the time domain, and it was found that the convergence characteristics were subject to eigenvalue distribution of the autocorrelation matrix of the filtered reference signal [4, 7]. Analysis in the time domain, however, requires a great deal of computation, and its physical meaning is unclear.

This chapter presents a new method for evaluating the adaptive algorithm for the feedforward ANC system, which can be approximately analysed in the frequency domain at each frequency (FFT) bin separately, which can provide significant computational savings and a better understanding of the physical meaning. Some convergence characteristics in the frequency domain can be understood easily, and a preprocessing method is proposed to improve the whole performance of the adaptive algorithm, especially when the reference pathssre unknown or measured in prior. Most contents of this chapter are based on the previous works [8-11].

The chapter is orgnized as follows. In section 2, the model of adaptive algorithm for multiple noises and multiple control points system is introduced in the time domain and the frequency domain, separately. Section 3 analyzes the convergence characteristics of some adaptive algorithms in the frequency domain, like the filtered-x LMS algorithm, the Delayed-x LMS, and the MEFX LMS algorithm, and the effects of the secondary path and the reference path on the convergence performance are analysed. Some results are represented by computer simulations in section 4.

2. A multiple noise source and multiple control point ANC system

Figure 1 shows a general ANC system for multiple noise sources and multiple control points. In Figure 1, I is the number of noise sources, K is the number of the reference sensors of the adaptive digital filter (ADF) array, which are finite impulse response (FIR) filters, M is the number of secondary sources, and L is the number of the control points (error sensors). Such a system will be referred to as CASE[I, K, M, L] in this chapter. Noises are recorded by K reference sensors and the impulse response of the reference paths are modelled with the

transfer matrix $\mathbf{B}(n)$. There are $M \times L$ different secondary paths (secondary path matrix) between all secondary sources and error sensors, and all secondary paths are assumed to be time invariant and are modelled as $\mathbf{C}(n)$. The outputs of the adaptive filter arrays are used to drive M secondary sensors to reduce the effect of noises at the error sensors as large as possible according to the estimated secondary paths and the recorded reference signals.

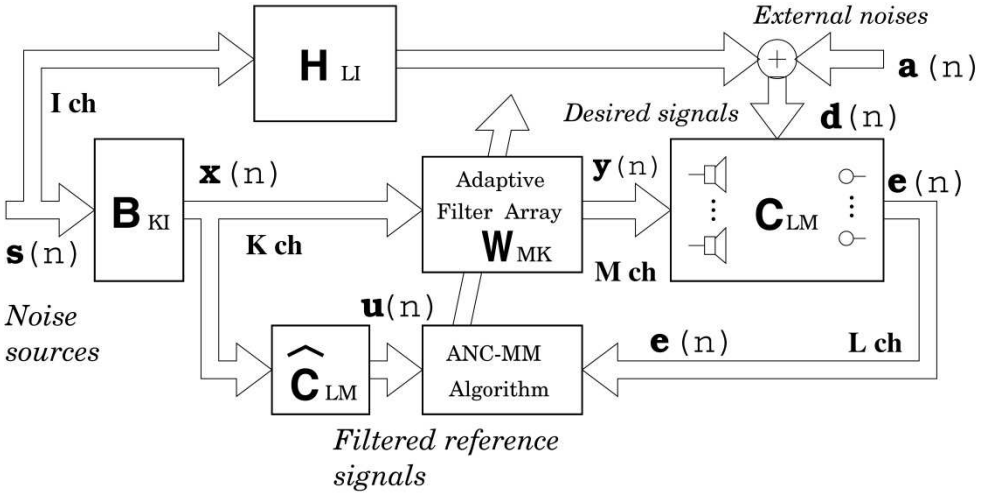

Fig. 1. Block diagram of the general active noise control system for multiple noise sources and multiple control points, CASE[I, K, M, L].

2.1 The adaptive algorithm in the time domain

As is shown in Figure 1, the adaptive controller generates the outputs to construct M secondary sources, and the squared sum of L error signals is minimized to update the coefficients of all adaptive filters. The updating mechanism of adaptive filter coefficients is controlled by the MEFX LMS algorithm, which is an extension of the filtered-x LMS algorithm for the CASE[I, K, M, L] ANC system.

The MEFX LMS algorithm can be summarized as follows [11],

$$\mathbf{e}(n) = \mathbf{d}(n) + \mathbf{U}(n)\mathbf{w}(n), \tag{1}$$

$$\mathbf{w}(n+1) = \mathbf{w}(n) - 2\mu\mathbf{U}^{\mathrm{T}}(n)\mathbf{e}(n), \tag{2}$$

where the superscript $^{\mathrm{T}}$ denotes the transpose, μ is the step-size parameter,

$$\mathbf{e}(n) = \left[e_1(n) \quad e_2(n) \quad \cdots \quad e_L(n)\right]^{\mathrm{T}}, \tag{3}$$

$$\mathbf{d}(n) = \left[d_1(n) \quad d_2(n) \quad \cdots \quad d_L(n)\right]^{\mathrm{T}} \tag{4}$$

and $\mathbf{w}(n)$ is the stacked column vector of all adaptive filter coefficients,

$$\mathbf{w}(n) = \left[\mathbf{w}_{11}(n) \quad \cdots \quad \mathbf{w}_{M1}(n) \quad \cdots \quad \cdots \quad \mathbf{w}_{MK}(n)\right]^{\mathrm{T}}. \tag{5}$$

The element of $\mathbf{w}(n)$, $\mathbf{w}_{mk}(n)$, is the adaptive filter coefficients vector between the *m*-th secondary source and the *k*-th reference signal,

$$\mathbf{w}_{mk}(n) = \left[\ w_{mk_1}(n) \quad w_{mk_2}(n) \quad \cdots \quad w_{mk_{N_w}}(n)\ \right], \tag{6}$$

where N_w is the length of the adaptive filters.

The filtered reference signal matrix $\mathbf{U}(n)$ is an $L \times MKN_w$ matrix and is defined by

$$\mathbf{U}(n) = \begin{bmatrix} \mathbf{u}_{111}^{\mathrm{T}}(n) & \mathbf{u}_{1M1}^{\mathrm{T}}(n) & \cdots & \mathbf{u}_{1MK}^{\mathrm{T}}(n) \\ \mathbf{u}_{211}^{\mathrm{T}}(n) & \mathbf{u}_{2M1}^{\mathrm{T}}(n) & \cdots & \mathbf{u}_{2MK}^{\mathrm{T}}(n) \\ \vdots & \vdots & \vdots & \vdots \\ \mathbf{u}_{L11}^{\mathrm{T}}(n) & \mathbf{u}_{LM1}^{\mathrm{T}}(n) & \cdots & \mathbf{u}_{LMK}^{\mathrm{T}}(n) \end{bmatrix}, \tag{7}$$

where the element of $\mathbf{U}(n)$, $\mathbf{u}_{lmk}(n)$, is the N_w-vector of the filtered reference signals

$$\mathbf{u}_{lmk}(n) = \left[u_{lmk}(n) \quad u_{lmk}(n-1) \quad \ldots \quad u_{lmk}(n-N_w+1)\right]^{\mathrm{T}}, \tag{8}$$

and the filtered reference signal $u_{lmk}(n)$ is obtained by

$$u_{lmk}(n) = \sum_{j=1}^{N_c} c_{lm_j}(n) x_k(n-j+1), \tag{9}$$

$$l = 1, \quad \cdots \quad L; \quad m = 1, \quad \cdots \quad M; \quad k = 1, \quad \cdots \quad K$$

where N_c is length of the estimated secondary path $\mathbf{c}_{lm} = \left[c_{lm_1} \quad c_{lm_2} \quad \ldots \quad c_{lm_{N_c}}\right]^{\mathrm{T}}$, which models the response between the *m*-th secondary source to the *l*-th error sensor. The reference signal $x_k(n)$ at the *k*-th reference sensor is

$$x_k(n) = \sum_{i=1}^{I} b_{ki} * s_i(n) = \sum_{i=1}^{I} \sum_{j_b=1}^{N_b} b_{kij_b}(n) s_i(n-j_b+1), \tag{10}$$

where $s_i(n)$ is the *i*-th noise source and $b_{ki}(n)$ is the impulse response from the *i*-th noise source to the *k*-th reference sensor, which is assumed to be a finite length of N_b.

2.2 Analysis in the time domain

It is well known that the convergence speed of the LMS algorithm is determined by the convergence time of different modes, which depend on the eigenvalues of the autocorrelation matrix, $E\left[\ \mathbf{x}(n)\mathbf{x}^{\mathrm{T}}(n)\ \right]$, of the input signals to adaptive filter [12-14]. Similar conclusion is applied to the MEFX LMS algorithm to analyse the eigenvalue spread of the autocorrelation matrix of the filtered reference signals [2], which is defined by

$$\mathbf{R}(n) = E[\ \mathbf{U}^{\mathrm{T}}(n)\mathbf{U}(n)\ ], \tag{11}$$

where $E[\ ]$ is the statistical expectation operator. The reference signals are assumed to be statistically stationary and time index n of the matrix $\mathbf{R}$ has been emitted.
To analyse the convergence characteristics of the MEFX LMS algorithm in the time domain, it is necessary to calculate the autocorrelation matrix $\mathbf{R}$ of the filtered reference signal, whose size is $MKN_w \times MKN_w$. Therefore, it is difficult to calculate the eigenvalues of the matrix $\mathbf{R}$ so as to investigate the convergence characteristics of the adaptive filters in the time domain. Another disadvantage is that the physical meanings of both maximum and minimum eigenvalues of the matrix $\mathbf{R}$ are unclear since the filtered reference signals include the reference paths and secondary paths by convolution operation.

2.3 Analysis in the frequency domain

In this section, the convergence characteristics of the MEFX LMS algorithm are analysed in the frequency domain. It is known that the system using the filtered-x LMS algorithm may be unstable, even for a very small step-size parameter (resulting in a slow adaptive speed), because small estimated errors to the secondary paths will enlarge the filtered reference signals to make the whole algorithm diverge in the time domain [2]. Since the convergence speed of the MEFX LMS algorithm is slow, the adaptive filters can be considered as time invariant linear filters for a short period. Thus, the MEFX LMS algorithm described in equations (1) and (2) in the time domain can be approximately expressed in the frequency domain as [10, 11]

$$\mathbf{E}(n,\omega) = \mathbf{D}(n,\omega) + \mathbf{U}(n,\omega)\mathbf{W}(n,\omega), \tag{12}$$

$$\mathbf{W}(n+1,\omega) = \mathbf{W}(n,w) - 2\mu\mathbf{U}^{\mathrm{H}}(n,\omega)\mathbf{E}(n,\omega), \tag{13}$$

where the superscript $^{\mathrm{H}}$ denotes the Hermitian transpose, and

$$\mathbf{E}(n,\omega) = [E_1(n,\omega),\quad E_2(n,\omega),\quad \cdots\quad E_L(n,\omega)]^{\mathrm{T}}, \tag{14}$$

$$\mathbf{D}(n,\omega) = [D_1(n,\omega),\quad D_2(n,\omega),\quad \cdots\quad D_L(n,\omega)]^{\mathrm{T}}, \tag{15}$$

$$\mathbf{W}(n,\omega) = [W_{11}(n,\omega),\quad \cdots\quad \cdots\quad W_{MK}(n,\omega)]^{\mathrm{T}}. \tag{16}$$

The filtered reference matrix $\mathbf{U}(n,\omega)$ is an $L \times MK$ matrix defined by

$$\mathbf{U}(n,\omega) = \begin{bmatrix} U_{111}(n,\omega) & \cdots & U_{1M1}(n,\omega) & \cdots & \cdots & U_{1MK}(n,\omega) \\ U_{211}(n,\omega) & \cdots & U_{2M1}(n,\omega) & \cdots & \cdots & U_{2MK}(n,\omega) \\ \vdots & \vdots & \vdots & \vdots & \vdots & \vdots \\ U_{L11}(n,\omega) & \cdots & U_{LM1}(n,\omega) & \cdots & \cdots & U_{LMK}(n,\omega) \end{bmatrix}, \tag{17}$$

where

$$U_{lmk}(n,\omega) = C_{lm}(\omega)X_k(n,\omega), \tag{18}$$

$C_{lm}(\omega)$ is the estimated transfer function from the *m*-th secondary source to the *l*-th error sensor, $X_k(n,\omega)$ is the reference signal obtained at the *k*-th reference sensor,

$$X_k(n,\omega) = \sum_{i=1}^{I} B_{ki}(n,\omega) S_i(n,\omega) \cdot \tag{19}$$

The matrix $\mathbf{R}(\omega)$ is defined by the matrix of the filtered reference signal $\mathbf{U}(n,\omega)$, as follows,

$$\mathbf{R}(\omega) = E\left[\ \mathbf{U}^{\mathrm{H}}(n,\omega)\mathbf{U}(n,\omega)\ \right] \cdot \tag{20}$$

In the time domain, the matrix $\mathbf{R}(n)$ shown in equation (11) is the autocorrelation matrix [13] . In the frequency domain, the matrix $\mathbf{R}(\omega)$ in equation (20) is called the power spectrum matrix. Since the dimensions of the power spectrum matrix $\mathbf{R}(\omega)$ are $MK \times MK$ at each frequency bin ω such that much less computation is required to find the eigenvalues of the matrix $\mathbf{R}(\omega)$ in the frequency domain than those in the time domain.

As is the same with the analysis in the time domain [12-14], the upper limit of the step-size parameter $\mu(\omega)$ and the longest time constant $\tau(\omega)$ can be given at each frequency bin by

$$0 < \mu(\omega) < \frac{1}{\lambda_{\max}(\omega)}, \tag{21}$$

$$\tau(\omega) > \frac{1}{2\mu(\omega)\lambda_{\min}(\omega)} \cdot \tag{22}$$

Where $\lambda_{\max}(\omega)$ and $\lambda_{\min}(\omega)$ are the largest and smallest eigenvalues of the matrix $\mathbf{R}(\omega)$ shown in equation (20) at each frequency bin. Over the whole frequency range of interest, the upper limit of the step-size parameter μ is given by

$$0 < \mu < \frac{1}{\max\limits_{\omega}\{\lambda_{\max}(\omega)\}} \cdot \tag{23}$$

Where $\max\limits_{\omega}\{\ \}$ denotes the maximum value over the whole frequency range. In practice, we can choose the unique step-size parameter determined by equation (23) to keep the system stable. Hence, smaller $\lambda_{\max}(\omega)$ leads to a slower convergence at some frequency bins. Especially, if a large sharp dip exists over the whole frequency range, the corresponding convergence speed will be slowed down. The sharper the dip becomes, the slower the convergence speed will be.

It was also found from simulation results [16] that the smaller $\lambda_{\max}(\omega)$ leads to a larger computational error and a smaller noise reduction at some frequency bins, results in a slow convergence speed over the entire frequency range, which is the same as in the time domain. Substituting equation (23) into equation (22) will give the longest time constant at each frequency bin, $\tau_{\max}(\omega)$, as follows,

$$\tau_{\max}(\omega) > \frac{\max\limits_{\omega}\{\lambda_{\max}(\omega)\}}{2\lambda_{\min}(\omega)}, \tag{24}$$

It is clear that the convergence speed is subject to the ratio of the maximum to the minimum eigenvalues.

It is clear from equation (24) that the convergence speed is subject to the minimum eigenvalue of the matrix $\mathbf{R}(\omega)$ at the frequency bin ω. Comparing the convergence speed of the adaptive filters at different frequency bin ω, it is found that a smaller eigenvalue of the power spectrum matrix $\mathbf{R}(\omega)$ results in a longer convergence time. Then, the convergence speed of the adaptive filters over the whole frequency bin (in the time domain) becomes slower.

The longest time constant, $\tau_{\max}$, over the whole frequency range can be obtained as

$$\tau_{\max} > \frac{\max\limits_{\omega}\{\lambda_{\max}(\omega)\}}{2\min\limits_{\omega}\{\lambda_{\min}(\omega)\}}, \tag{25}$$

where $\min\limits_{\omega}\{\ \}$ denotes the minimum values over the whole frequency range. It is clear from equation (25) that the longest time constant is related to the ratio of the maximum to the minimum eigenvalue of the matrix $\mathbf{R}(\omega)$ over the whole frequency range. The convergence analysis of the time domain MEFX LMS algorithm may be evaluated generally in the frequency domain such that we can obtain insight into the convergence characteristics of the MEFX LMS algorithm in the time domain.

2.4 The power spectrum matrix R

The filtered reference signal $u(n)=\sum_{i=1}^{N_c} x(n-i+1)c_i$ in the time domain is expressed by the convolution of $x(n)$ and $c(n)$, while $U(n,\omega)=C(\omega)X(n,\omega)$ in the frequency domain is expressed by a simple multiplication. Rearrange the filtered reference matrix $\mathbf{U}(n,\omega)$ in equation(17) and combine the result of equation (18), the matrix $\mathbf{U}(n,\omega)$ can be written as

$$\mathbf{U}(n,\omega)=\mathbf{X}^{\mathrm{T}}(n,\omega)\otimes\mathbf{C}(\omega), \tag{26}$$

where $\otimes$ is the Kronecker product, and

$$\mathbf{X}(n,\omega)=\mathbf{B}(\omega)\mathbf{S}(n,\omega), \tag{27}$$

where the reference path $\mathbf{B}(\omega)$ and the secondary path $\mathrm{C}(\omega)$ are

$$\mathbf{C}=\begin{bmatrix} C_{11} & C_{12} & \cdots & C_{1M} \\ C_{21} & C_{22} & \cdots & C_{2M} \\ \cdots & \cdots & \cdots & \cdots \\ C_{L1} & C_{L2} & \cdots & C_{LM} \end{bmatrix} \quad \text{and} \quad \mathbf{B}=\begin{bmatrix} B_{11} & B_{12} & \cdots & B_{1I} \\ B_{21} & B_{22} & \cdots & B_{2I} \\ \cdots & \cdots & \cdots & \cdots \\ B_{K1} & B_{K2} & \cdots & B_{KI} \end{bmatrix}.$$

The matrix $\mathbf{R}(\omega)$ can be given by

$$\mathbf{R}(\omega)=E[\mathbf{U}^{\mathrm{H}}(n,\omega)\mathbf{U}(n,\omega)]=E\{[\mathbf{X}^{\mathrm{T}}(n,\omega)\otimes\mathbf{C}(\omega)]^{\mathrm{H}}[\mathbf{X}^{\mathrm{T}}(n,\omega)\otimes\mathbf{C}(\omega)]\} \tag{28}$$

Utilizing the Kronecker product characteristics,

$$\begin{aligned}\mathbf{R}(\omega) &= E\{[\mathbf{X}^{\mathrm{T}}(n,\omega)\otimes\mathbf{C}(\omega)]^{\mathrm{H}}[\mathbf{X}^{\mathrm{T}}(n,\omega)\otimes\mathbf{C}(\omega)]\}\\ &= [E\{\mathbf{X}(n,\omega)\mathbf{X}^{\mathrm{H}}(n,\omega)\}]^{*}\otimes[\mathbf{C}^{\mathrm{H}}(\omega)\mathbf{C}(\omega)]\\ &= [\mathbf{B}(\omega)E\{\mathbf{S}(n,\omega)\mathbf{S}^{\mathrm{H}}(n,\omega)\}\mathbf{B}^{\mathrm{H}}(\omega)]^{*}\otimes[\mathbf{C}^{\mathrm{H}}(\omega)\mathbf{C}(\omega)]\\ &= |s_1|^2\ldots|s_I|^2[\mathbf{B}(\omega)\mathbf{B}^{\mathrm{H}}(\omega)]^{*}\otimes[\mathbf{C}^{\mathrm{H}}(\omega)\mathbf{C}(\omega)]\end{aligned} \tag{29}$$

$MK\times MK$ power spectrum matrix $\mathbf{R}(\omega)$ is dependent completely on the reference path $\mathbf{B}(\omega)$ and the secondary path $\mathbf{C}(\omega)$.

It is easy to prove that $\mathbf{R}(\omega)$ is Hermitian matrix, i.e. $\mathbf{R}(\omega)=\mathbf{R}^{\mathrm{H}}(\omega)$, so all eigenvalues of $\mathbf{R}(\omega)$ are nonnegative, that is to say, $\mathbf{R}(\omega)$ is a nonnegative define matrix. $\mathbf{B}(\omega)\mathbf{B}^{\mathrm{H}}(\omega)$ and $\mathbf{C}^{\mathrm{H}}(\omega)\mathbf{C}(\omega)$ are also Hermitian. According to the characteristics of the Kronecker product, the determinant and trace of $\mathbf{R}(\omega)$ satisfy the following equations

$$\det[\mathbf{R}(\omega)] = \det[\mathbf{C}^{\mathrm{H}}(\omega)\mathbf{C}(\omega)]^{K}\det[\mathbf{B}(\omega)\mathbf{B}^{\mathrm{H}}(\omega)]^{M} \tag{30}$$

$$Trac[\mathbf{R}(\omega)] = Trac[\mathbf{C}^{\mathrm{H}}(\omega)\mathbf{C}(\omega)]Trac[\mathbf{B}(\omega)\mathbf{B}^{\mathrm{H}}(\omega)] \tag{31}$$

The determinant of the power spectrum matrix $\mathbf{R}(\omega)$ may be expressed in terms of the input power spectra $|s_1|^2,\cdots,|s_I|^2$, K times the determinant of the matrix $\mathbf{C}^{\mathrm{H}}(\omega)\mathbf{C}(\omega)$ and M times determinant of the matrix $\mathbf{B}(\omega)\mathbf{B}^{\mathrm{H}}(\omega)$.

From equation (25), the longest time constant $\tau_{\max}$ is only determined by the ratio of the maximum and minimum eigenvalues of $\mathbf{R}(\omega)$, so the $\tau_{\max}$ is independent of the noise power $|S_1|^2,\cdots,|S_I|^2$ and only determined by the characteristic of the reference path $\mathbf{B}(\omega)$ and the secondary path $\mathbf{C}(\omega)$. In general, if the determinant of the matrix $\mathbf{C}^{\mathrm{H}}(\omega)\mathbf{C}(\omega)$ or $\mathbf{B}(\omega)\mathbf{B}^{\mathrm{H}}(\omega)$ is small, the smallest eigenvalue of the matrix $\mathbf{C}^{\mathrm{H}}(\omega)\mathbf{C}(\omega)$ or $\mathbf{B}(\omega)\mathbf{B}^{\mathrm{H}}(\omega)$ is small, and the smallest eigenvalue of the matrix $\mathbf{R}(\omega)$ is also small. Therefore, the convergence characteristics of the MEFX LMS algorithm can be evaluated separately by the distributions of eigenvalues of the matrix $\mathbf{C}^{\mathrm{H}}(\omega)\mathbf{C}(\omega)$ or $\mathbf{B}(\omega)\mathbf{B}^{\mathrm{H}}(\omega)$.

3. The behavior of adaptive algorithm in the frequency domain

3.1 The filtered-x LMS algorithm

Firstly, Let us investigate the convergence characteristics of the filtered-x algorithm influenced by the secondary path C for a simple ANC system, CASE[1,1,1,1]. For convenience, assuming that the primary noise s(n) is white noise with zero mean and unit variance ($\sigma^2=1$), and the primary path b(n) is 1, so

$$X(n,\omega) = B(\omega)S(n,\omega) = S(n,\omega). \tag{32}$$

In the CASE[1,1,1,1], a simple ANC system, the power spectrum $\mathbf{R}(\omega)$ is real at each frequency bin ω

$$R(\omega) = |S_1|^2 |C(\omega)|^2 |B(\omega)|^2$$

In this case, $R(\omega)$ can be expressed as follows:

$$R(\omega) = |S_1|^2 |C(\omega)|^2 |B(\omega)|^2 = \sigma^2 |C(\omega)|^2 |B(\omega)|^2 = |C(\omega)|^2, \tag{33}$$

and the upper limit of the step-size parameter μ from equation (21) can be rewritten as

$$\mu < \frac{1}{\max\limits_{\omega}\{|C(\omega)|^2\}}, \tag{34}$$

It is clear that the step-size parameter μ is subject to the maximum value of $|C(\omega)|^2$. The time constant, $\tau(\omega)$, at a frequency bin can be obtained from equation (22), as

$$\tau(\omega) \approx \frac{1}{2\mu|C(\omega)|^2}, \tag{35}$$

$$t(\omega) > \frac{\max\left\{|C(\omega)|^2\right\}}{2|C(\omega)|^2}. \tag{36}$$

It is found from equation (35) that the smaller value of $|C(\omega)|^2$ leads to a slower convergence speed of the adaptive filter at the frequency bin ω. In other words, if $|C(\omega)|^2$ shows a large dip at a frequency bin ω, the convergence speed of the adaptive filter is slow at that frequency bin, and the total convergence speed is also slow. This means that the performance of the filtered-x LMS algorithm is not good if the power gain of the secondary path C is not flat over the whole frequency range. In practical cases, the transfer function of the secondary path C has to be measured prior to the active noise cancelation. Therefore, the convergence characteristics can be evaluated by the power gain of the measured secondary path C.

With the secondary path C measured experimentally or generated by computer, the simulations show that the smaller value of the power gain of the secondary path C leads to slower a convergence speed, a larger computation error and a smaller cancellation at a given frequency bin.

3.2 The delayed-x LMS algorithm

The filtered-x LMS algorithm is widely used in feedforward ANC systems. This adaptive algorithm is an alternate version of the LMS algorithm when the secondary path C from the adaptive filter output to the error sensor is represented by a non-unitary transfer function. The Filtered-x LMS algorithm requires a filtered reference signal, which are the convolution of the reference signal and the impulse response of a secondary path C. As a result, this algorithm has a heavy computational burden for real-time controllers.

The Delayed-x LMS algorithm [9] is a simplified form of the filtered-x LMS algorithm, where the secondary path C from the secondary source to the error sensor is represented

by a pure delay of k samples (the delayed model D) to reduce computation and system complexity. This simplified version has been applied in telecommunications applications [16,17]. In the ANC system, the simplification will bring a modelling error [18,19], which causes deterioration in the ANC performance. The ANC system with the Delayed-x LMS algorithm was empirically studied in the time domain [20-22], and stability has been evaluated by using a frequency domain model of the ''filtered'' LMS algorithm [23]. The theoretical study of the convergence characteristics will be summarized here.

In the Delayed-x LMS algorithm, the model of the secondary path C is replaced by a delayed model D, and no convolution is required to obtain the filtered reference signal. A block diagram of the ANC system with the Delayed-x LMS algorithm is shown in Figure 2. The filtered reference signal is given by

$$u'(n) = gx(n-k) \tag{37}$$

where the gain g is usually 1 and k is the number of points from 0 to the peak of the impulse response of the secondary path C.

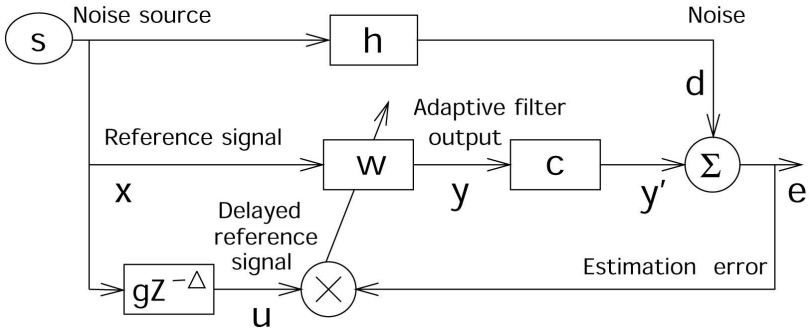

Fig. 2. Block diagram of an ANC system with the Delayed-x LMS algorithm.

The Delayed-x LMS algorithm can reduce computation loading significantly by eliminating the convolution. However, the modelling error caused by simplifying the filtered reference signal deteriorates the performance of the adaptive control system. In the frequency domain, $U(\omega,n)$ is the DFT of the filtered reference signal $u(n)$ filtered by the real secondary path, $U(\omega,n) \approx X(\omega,n)C(\omega)$. $U'(\omega,n)$ is the DFT of the filtered reference signal $u'(n)$ in equation (37), $U'(\omega,n) \approx X(\omega,n)G(\omega)$ and $\overline{U'(\omega,n)}$ is the complex conjugate of $U'(\omega,n)$. The transfer function of the delayed model D is defined as $G(\omega)$. From equation (20), the convergence characteristics of the Delayed-x LMS algorithm are defined by matrix $E[\overline{U'(\omega,n)}U(\omega,n)]$ at each frequency bin ω. Assuming that the primary noise $s(n)$ is a white noise with zero mean and unit variance, the matrix can be written as

$$E[\overline{U'(\omega,n)}U(\omega,n)] = E[\overline{G(\omega)}C(\omega)] \tag{38}$$

It is clear that the stability of the Delayed-x LMS algorithm is assured by

$$0 < \left|1 - 2\mu\overline{G(\omega)}C(\omega)\right| < 1, \tag{39}$$

where

$$\overline{G(\omega)} = |G(\omega)|\exp(-j\theta_g(\omega)), \tag{40}$$

$$C(\omega) = |C(\omega)|\exp(j\theta_c(\omega)), \tag{41}$$

and $\theta_g(\omega)$ and $\theta_c(\omega)$ are phases of $G(\omega)$ and $C(\omega)$, respectively. For convenience, the frequency bin ω will be omitted hereafter. From equations (40) and (41), equation (39) can be rewritten as

$$0 < \left|1 - 2\mu|G||C|\exp(j(\theta_c - \theta_g))\right| < 1 \tag{42}$$

It is clear that the change of the gain $|G|$ can be included into the adjustment of the step-size parameter μ. The stability condition of the Delayed-x LMS algorithm is determined by the phase error $\theta_s = \theta_c - \theta_g$ in the following range

$$-\pi/2 < \theta_s (\mathrm{mod}\, 2\pi) < \pi/2 . \tag{43}$$

In other words, if the phase error θ_s is out of the above range, the Delayed-x LMS algorithm will not be stable. The theoretical result in equation (43) is the same as that obtained by Feinutuch [23]. For easy understanding, the stability and convergence characteristics of the Delayed-x LMS algorithm are also discussed in the complex plane [9, 24]. It is found the Delayed-x LMS algorithm is stable when the phase error will keep in the range between $-\pi/2$ and $-\pi/2$. It is also found that the convergence speed of the adaptive filter is slower and cancellation is smaller when the phase error with the stability condition in equation (43) is large in the frequency domain.

Since the secondary path C can be measured generally prior to active cancellation, stability and convergence characteristics are easily evaluated by calculation the phase error before cancellation. A possible way to achieve good performance is to adjust the position of the loudspeaker and error microphone or to adjust the number of delayed points.

3.3 The behavior of the multichannel filtered-x algorithm

In this section, the behavior of the MEFX LMS algorithm will be evaluated in CASE[I,K,L,M] system with $M \times L$ secondary paths $\mathbf{C}$ and $K \times I$ reference paths $\mathbf{B}$. As stated in equation (29), the power spectrum matrix $\mathbf{R}(\omega)$ is determined by the secondary paths $\mathbf{C}(\omega)$ and the reference paths $\mathbf{B}(\omega)$. The effect of $\mathbf{C}(\omega)$ and $\mathbf{B}(\omega)$ on the convergence behavior of the MEFX LMS algorithm will be discussed separately, and a new preprocessing method to the reference path is proposed to improve the whole performance of the adaptive algorithm.

3.3.1 The matrix C

In general, if the smallest eigenvalue of the matrix $\mathbf{R}$ is small, the smallest eigenvalue of the matrix $\mathbf{C}^{\mathrm{H}}\mathbf{C}$ is small, so the determinant of the matrix $\mathbf{C}^{\mathrm{H}}\mathbf{C}$ is also small. An approximate method to avoid computing the eigen-decomposition of $\mathbf{C}^{\mathrm{H}}\mathbf{C}$ is to replace the ratio of the maximum to minimum eigenvalue with the ratio of determinant. Define the ratio $\rho(\omega)$ instead of equation (25) as follows,

$$\rho_C(\omega) = \frac{\max_{\omega}\{\left|\mathbf{C}^H(\omega)\mathbf{C}(\omega)\right|\}}{\left|\mathbf{C}^H(\omega)\mathbf{C}(\omega)\right|}. \tag{44}$$

The ratio $\rho_C(\omega)$ of the maximum to the minimum value of the determinant of matrix $\mathbf{C}^H\mathbf{C}$ over the whole frequency range is defined by

$$\rho_C = \frac{\max_{\omega}\{\left|\mathbf{C}^H(\omega)\mathbf{C}(\omega)\right|\}}{\min_{\omega}\{\left|\mathbf{C}^H(\omega)\mathbf{C}(\omega)\right|\}}. \tag{45}$$

Thus, we can evaluate the convergence speed approximately by using the ratio ρ_C, instead of calculating the eigenvalues of the matrix $\mathbf{R}$ or $\mathbf{C}^H\mathbf{C}$. This is to say, the frequency domain analysis requires much less computation compared with the time domain analysis. The physical meaning of the matrix $\mathbf{C}^H\mathbf{C}$ will be further discussed in the next section.

3.3.2 The physical meaning

The physical meaning of the matrix $\mathbf{C}^H\mathbf{C}$ will be discussed in detail in this section. For simplicity, an $M = L = 2$ system will be considered, of course equation $\left|\mathbf{C}^H\mathbf{C}\right| = \left|\mathbf{C}\right|^2$ is valid in this case. At each frequency bin ω, the matrix $\mathbf{C}$ can be expressed by

$$\mathbf{C} = \begin{bmatrix} C_{11} & C_{12} \\ C_{21} & C_{22} \end{bmatrix}. \tag{46}$$

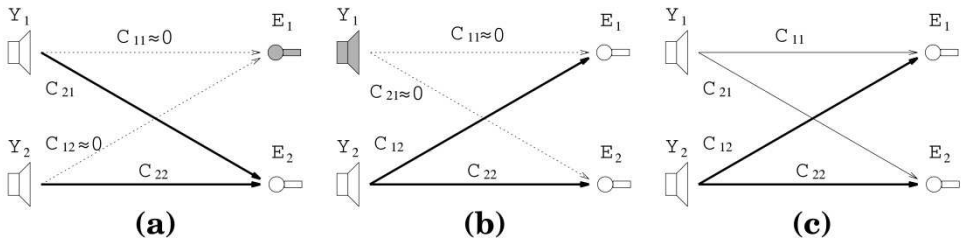

Fig. 3. The condition for $\left|\mathbf{C}\right| \approx 0$, in the case of an $M = L = 2$.

Referring to Figure 3, at a frequency bin ω, the determinant of the matrix is small ($\left|\mathbf{C}\right| \approx 0$) in the following three cases: (a) All elements of a row of the matrix $\mathbf{C}$ are small (e.g., $C_{11} \approx 0$ and $C_{12} \approx 0$), which implies the existence of a common zero in the transfer function of secondary paths from two secondary sources to the error sensor 1; (b) All elements of a column of the matrix $\mathbf{C}$ are small (e.g., $C_{11} \approx 0$ and $C_{12} \approx 0$), which means the secondary source 1 does not work at this frequency. Hence, the effective number of secondary sources is decreased. (c) The transfer paths from the secondary sources to the error sensors are similar. This can be expressed mathematically as

$$C_{11} / C_{21} \approx C_{12} / C_{22}. \tag{47}$$

It follows from equation (47) that two secondary sources act as one secondary source. This means that the effective number of the secondary sources is decreased. Therefore, the multiple channel ANC system does not work properly. It is well known that characteristics of the secondary paths are dependent upon the arrangement of secondary sources / error sensors, as well as frequency responses. Therefore, if the frequency responses of the secondary sources to the error sensors are proportional as equation (47), which implies that either the secondary sources or the error sensors will be located close to each other, which reduces the effective number of secondary sources. On the other hand, in practical applications, frequency responses of the secondary sources to the error sensors are frequently different at each frequency bin. Under this condition, even if their arrangement is not close together as y mentioned above, equation (47) may be valid, which results in a divergence of the adaptive process. In summary, either arrangement of the secondary sources to the error sensors, or their frequency responses can make equation (47) valid, the determination of matrix $\mathbf{C}$ may be equal approximately to zero and the eigenvalue spread of the power spectrum matrix $\mathbf{R}$ will become large.

For the three cases mentioned above, since $|\mathbf{C}|$ or $|\mathbf{C}^{\mathrm{H}}\mathbf{C}|$ is small, the smallest eigenvalue of the power spectrum matrix $\mathbf{R}$ is correspondingly small, which results in a low convergence speed. If the value $|\mathbf{C}^{\mathrm{H}}\mathbf{C}|$ varies significantly over the whole frequency range, the convergence speed of the MEFX LMS algorithm is also slow. From the previous works on the single-channel ANC system, conditions (a) and (b) can easily be considered. However, such conditions are very rare in practical applications. Condition (c), which occurs more frequently in practical applications, should be emphasized in a practical ANC system for multiple control points. The physical meaning of the general multiple channel ANC system can be discussed by using the rank and the linear independence theory of the matrix $\mathbf{C}$.

In practical applications, since the transfer function for the secondary paths, which is time invariant in most cases, can be measured prior to the ANC processing, the influence of multiple secondary paths on the convergence speed should be evaluated prior to the ANC processing.

3.4 The matrix B

In equation (29), the transfer function matrix $\mathbf{B}$ of the reference paths is similar to the transfer matrix $\mathbf{C}$ of the secondary paths, so that the characteristics of the matrix $\mathbf{C}$ are also similar to those of matrix $\mathbf{B}$. But the physical meaning of smaller $|\mathbf{B}|$ is different that of $|\mathbf{C}|$.

Here, the physical meaning of the case that $|\mathbf{B}\mathbf{B}^{\mathrm{H}}| \approx 0$ is discussed for an $I = K = 2$ system for simplicity. The equation $|\mathbf{B}\mathbf{B}^{\mathrm{H}}| = |\mathbf{B}|^2$ is valid in this case.

For each frequency bin ω, $\mathbf{B}$ is of the form

$$\mathbf{B} = \begin{bmatrix} B_{11} & B_{12} \\ B_{21} & B_{22} \end{bmatrix} \tag{48}$$

Referring to Figure 4, at a frequency bin ω, the determinant of the matrix is small ($|\mathbf{B}| \approx 0$) in the following three cases:

a. All elements of a row of the matrix $\mathbf{B}$ are small (e.g., $B_{11} \approx 0$ and $B_{12} \approx 0$). This implies the existence of a common zero in the transfer function from two noise sources to the reference sensor #1.
b. All elements of a column of the matrix $\mathbf{B}$ are small (e.g., $B_{11} \approx 0$ and $B_{21} \approx 0$). In this case, noise source #1 doesn't exist at this frequency. Hence, the reference sensor cannot receive the correct reference signal from noise source #1.
c. The transfer rates from the noise sources to the reference sensors are similar ($B_{11} / B_{21} \approx B_{12} / B_{22}$). In this case, $X_2 \approx (B_{21} / B_{11}) X_1$, and this is equivalent to using only one reference sensor at this frequency, even though two sensors are used. This means that the effective number of the reference sensors is decreased, and perfect noise cancellation is impossible. But minimization of the noise level is achievable in the sense of the least mean square error by the adaptive processing of the ANC system. Therefore, the multiple channel ANC system does not work properly.

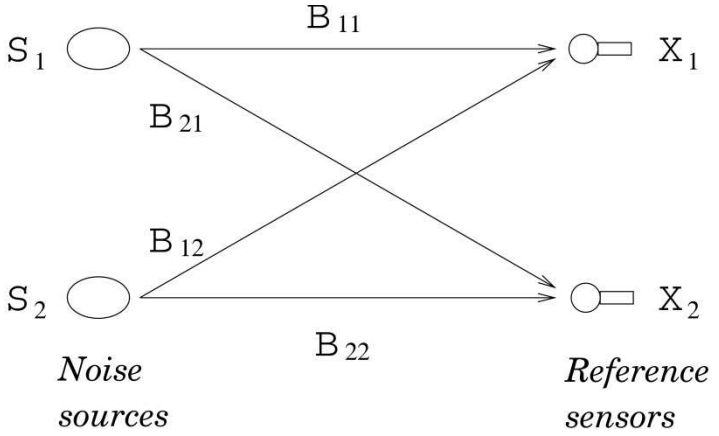

Fig. 4. Block diagram for 2 noise sources and 2 reference sensors.

For the three cases mentioned above, the value of the determinant of the matrix $|\mathbf{B}|$ or $|\mathbf{B}\mathbf{B}^{\mathbf{H}}|$ become small, and the physical meaning is the correlation between the reference signals X_1 and X_2 become large [24]. In this case, the determinant or the smallest eigenvalue of the matrix $|\mathbf{B}|$ is small, the smallest eigenvalue of the power spectrum matrix $\mathbf{R}$ is also small, and the convergence speed of the adaptive filters is slow at that frequency bin. Then, the convergence speed of the mean square error at the error sensors is also slow. If the value $|\mathbf{B}\mathbf{B}^{\mathrm{H}}|$ varies over the whole frequency range, the convergence speed of the MEFX LMS algorithm is slower.

It is analysed from equation (29) that exchanging the roles of the transfer matrices $\mathbf{B}$ and $\mathbf{C}$, the same conclusion can be obtained as in section 3.3.

An adaptive blind method for reducing the eigenvalue spread of the correlation matrix of reference signals is discussed in next section. The preprocessed outputs used as input of an ANC system are approximately uncorrelated noises and the power spectrums are flat approximately. The MEFX LMS algorithm converges rapidly and a small MSE is obtained [25, 26].

3.5 Blind preprocessing method for multichannel freedforward ANC system

Sometimes, the effects of the reference path $\mathbf{B}$ can't be ignored, especially when the reference sensors cannot be located near the noise sources. As stated in equation (30), the value $\left|\mathbf{B}\mathbf{B}^{\mathbf{H}}\right|$ at each frequency bin ω affects the eigenvalue spread of the autocorrelation matrices $\mathbf{R}$, and the step size μ and the longest time constant of the adaptive filter. In order to improve the whole performance of the MEFX LMS algorithm, some necessary preprocessing methods are proposed to reduce the effects of the reference path. However, noise signals are often unknown and time-varying in practice, and the accurate transfer function of the reference path is difficult to be measured in prior, so it seems impossible to cancel this effects. A blind preprocessing method is proposed to deal with this case, where noises are assumed to be independent or uncorrelated each other and the channel impulse responses are unknown.

An arbitrary linear system can be factored into the product of an all-pass system and a minimum phase system

$$\mathbf{B}(\omega) = \mathbf{B}_{min}(\omega)\mathbf{B}_{all}(\omega), \tag{49}$$

where the all-pass system satisfy $\mathbf{B}_{all}(\omega)\mathbf{B}_{all}^{\mathrm{H}}(\omega) = \mathbf{I}$, and the minimum phase component $\mathbf{B}_{min}(\omega)$ has a stable inverse. $\mathbf{B}(\omega)\mathbf{B}^{\mathrm{H}}(\omega)$ can be simplified as

$$\mathbf{B}(\omega)\mathbf{B}^{\mathrm{H}}(\omega) = \mathbf{B}_{min}(\omega)\mathbf{B}_{min}^{\mathrm{H}}(\omega)\,, \tag{50}$$

In order to eliminate or reduce the eigenvalue spread of $\mathbf{B}(\omega)\mathbf{B}^{\mathrm{H}}(\omega)$, a natural choice is to find an inverse system matrix $\mathbf{V}(\omega)$ to filter the reference signals, and the new transfer system matrix from the noise sources to the inputs of the adaptive filter array is $\mathbf{G}(\omega) = \mathbf{V}(\omega)\mathbf{B}(\omega)$, which has a smaller eigenvalue spread. The correlation matrix of the new system is

$$\mathbf{V}(\omega)\mathbf{B}(\omega)\mathbf{B}^{\mathrm{H}}(\omega)\mathbf{V}^{\mathrm{H}}(\omega) = \mathbf{V}(\omega)\mathbf{B}_{min}(\omega)\mathbf{B}_{min}^{\mathrm{H}}(\omega)\mathbf{V}^{\mathrm{H}}(\omega), \tag{51}$$

and the optimal inverse system matrix is $\mathbf{V}(\omega) = \mathbf{B}_{min}^{-1}(\omega)$.

If the reference path $\mathbf{B}(\omega)$ can be measured in prior, the optimal inverse system $\mathbf{V}(\omega)$ can be computed easily and fixed into the application to cancel the effect of the reference path. However, $\mathbf{B}(\omega)$ cannot be obtained in most applications in prior and may be time-varying in complicated application, an adaptive algorithm to find the optimal inverse system is expected. A blind spatial-temporal decorrelation algorithm is proposed in [25], which is based on maximization of entropy function in the time domain. More details and the final performance evaluation of the adaptive algorithm can be referred in [25, 26]. Computer simulations show that blind preprocessing algorithm can obtain lower MSE for multichannel feedforward ANC system.

4. Computer simulations

Numerical simulations are carried out to demonstrate the convergence characteristics discussed above by using a simple CASE[2, 2, 2, 2] system, as shown in Figure 5. All simulations are performed in the time domain, but their evaluation is carried out both in the time and frequency domains.

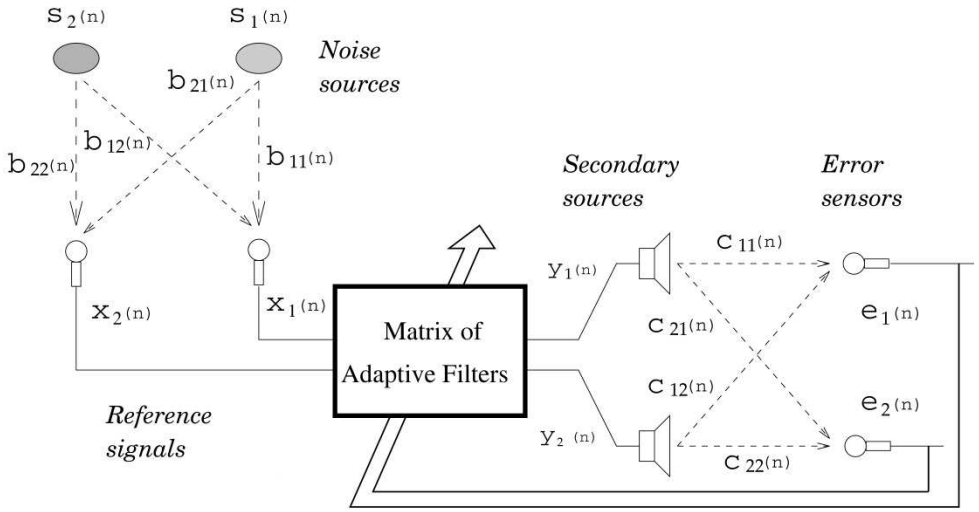

Fig. 5. Block diagram for CASE[2,2,2,2] ANC system.

For convenience, the experimental conditions are assumed as follows: (1) Noise sources $s_1(n)$ and $s_2(n)$ are uncorrelated white noise with zero mean and unit variance. (2) The responses of the primary paths H_{11}, H_{12}, H_{21}, and H_{22}, and the secondary paths C_{11}, C_{12}, C_{21}, and C_{22} are experimentally obtained in an ordinary room. (3) In order to evaluate the influence of the matrix **C**, the filtered reference signal $x_1(n) = s_1(n)$ and $x_2(n) = s_2(n)$ are selected. In this case, **B** = **I**, where **I** is the identity matrix.

The simulation is carried out by using four secondary paths as shown in Figure 6. The step-size parameter μ is set to 0.00001 to keep the system stable and achieve a better convergence.

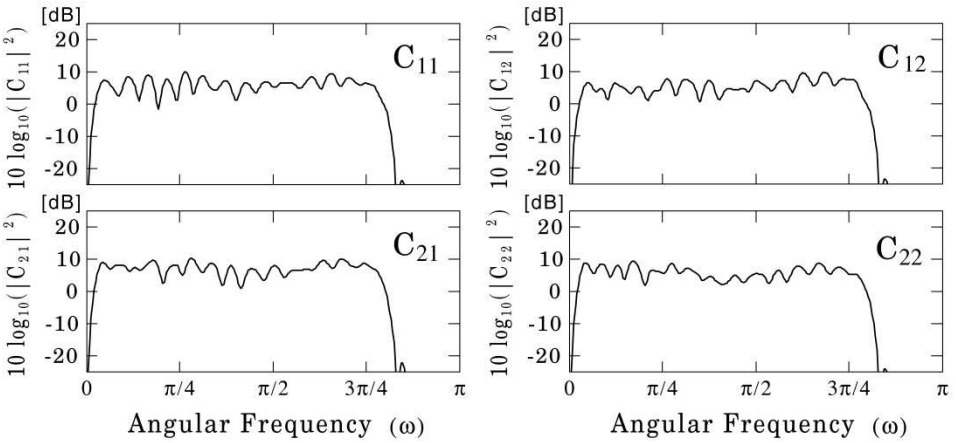

Fig. 6. The four transfer functions from the secondary sources to the error sensors.

There is no common zero in the four secondary paths C_{11}, C_{12}, C_{21}, and C_{22}, as shown in Figure 6. However, it can be seen from Figure 7(a) that there are some dips in the determinant of the matrix $\mathbf{C}^{\mathrm{H}}\mathbf{C}$. The two eigenvalues of the matrix $\mathbf{C}^{\mathrm{H}}\mathbf{C}$ are plotted in Figure 7(b). As can be seen from Figure 7, when the $\left|\mathbf{C}^{\mathrm{H}}\mathbf{C}\right|$ is small, the eigenvalues of the matrix $\mathbf{C}^{\mathrm{H}}\mathbf{C}$ are also small. Spectra of the residual signal at different iterations at the error sensor #1 are plotted in Figure 8. Nearly the same results are obtained at the error sensor #2, but these Figures are omitted in this chapter. Comparing Figures 7 and 8, if the $\left|\mathbf{C}^{\mathrm{H}}\mathbf{C}\right|$ at some frequencies is small, the residual power at the corresponding frequencies is high. In actual application, since the secondary paths, which is time invariant in most cases, should be measured prior to the ANC processing, the influence of the secondary path(s) on the convergence speed can be evaluated prior to the ANC processing. It is possible to make $\left|\mathbf{C}^{\mathrm{H}}\mathbf{C}\right|$ over the whole range flat by adjusting the locations of the secondary sensors and the error sensors.

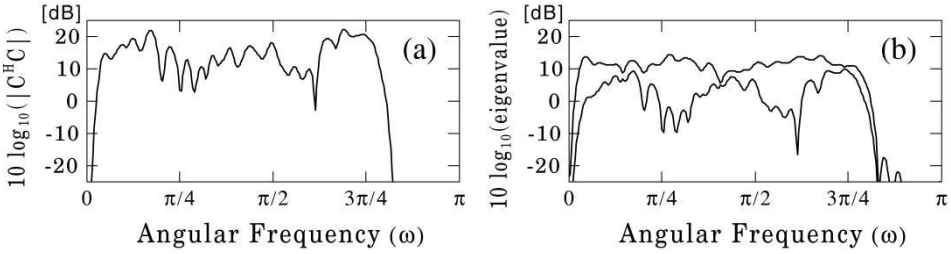

Fig. 7. The matrix $\mathbf{C}$ is composed of four secondary paths shown in Figure 6. (a): the determinant of the matrix $\mathbf{C}^{\mathrm{H}}\mathbf{C}$, $\left[10\log_{10}\left(\left|\mathbf{C}^{\mathrm{H}}\mathbf{C}\right|\right)\right]$ (b): two eigenvalues of the matrix $\mathbf{C}^{\mathrm{H}}\mathbf{C}$, $\left[10\log_{10}\left(eigenvalue\right)\right]$.

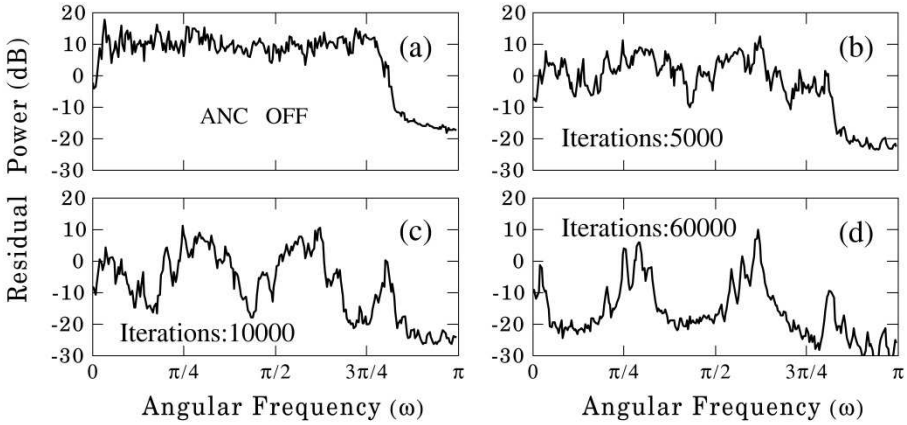

Fig. 8. Simulated power spectra of the residual noise (average of 20 times) at the error sensor #1, in the case of CASE[2,2,2,2] ANC system, when (B = I) . (a) Before adaptive processing; (b), (c) during adaptive processing, the numbers of the adaptive iterations are 5000 and 10000, respectively; (d) after adaptive processing, the number of the adaptive iterations are 60000. Similar results were obtained at the error sensor #2.

5. Conclusions

This chapter has shown that the convergence characteristics of the filtered-x LMS algorithm, the Delayed-x LMS algorithm and the MEFX LMS algorithm in the time domain could be analysed in the frequency domain with much less computation and a better understanding of the physical meaning. Through their analysis in the frequency domain instead of time domain, the convergence characteristics are subject to the eigenvalues of the power spectrum matrix $\mathbf{R}$, whose size is much smaller than that in the time domain. Another advantage is that the determinant of the power spectrum matrix $\mathbf{R}$ can be expressed by the product of the input spectra and the determinant of the matrix $\mathbf{C}^{H}\mathbf{C}$ and $\mathbf{B}\mathbf{B}^{H}$ in each frequency bin. The effect of multiple secondary paths has been investigated in detail in the case of the time invariant. It is found that the convergence characteristics of the MEFX LMS algorithm are affected by the determinant of $\mathbf{C}^{H}\mathbf{C}$, or the smallest eigenvalues of $\mathbf{C}^{H}\mathbf{C}$. However, since the transfer matrix $\mathbf{B}$ generally can't be measured prior to ANC cancellation, it is necessary to consider the influence of the correlation among the output of the reference sensors, which can be measured prior to ANC application. If the correlation among the output of the reference sensors is small over the whole frequency range, the convergence speed becomes fast. Simulation on the time-domain MEFX algorithm has been carried out and its convergence characteristics are evaluated in the frequency domain.

6. References

[1] Nelson, P. A., & Elliott, S. J. (1992). *Active Control of Sound,* Academic Press Inc. San Diego, Canada.

[2] Elliott, S. J., & Nelson, P. A. (1993). Active Noise Control, *IEEE signal processing magazine*, October 12-35.

[3] Elliott, S, (2001). Signal processing for active control, Academic Press, London.

[4] Widrow, B., & Stearns, S. D. (1985). *Adaptive Signal Processing,* Prentice-Hall Inc.

[5] Burgess, J.C. (1981). Active adaptive sound control in a duct: A computer simulation, *J. Acoust. Soc. Am.*, 70(3), pp. 715-726.

[6] Elliott, S. J., Stothers, I. M., & Nelson, P. A. (1987). A multiple error LMS algorithm and its application to active control of sound and vibration, proc. *IEEE Trans. Speech Audio Processing*, ASSP-35(10), pp.1423-1434.

[7] Elliott, S. J., & Boucher, C. C. (1994). Interaction between multiple feedforward active control system. *IEEE Trans. Acoustic. Speech Signal Process on speech and audio processing*, SAP-2 (4), pp.521-530.

[8] Chen, G., Abe, M., & Sone, T. (1995). Evaluation of the convergence characteristic of the filtered-x LMS algorithm in frequency domain, *J. Acoust. Soc. Jpn (E)*, 16(6), pp.331-340.

[9] Chen, G., Sone, T., Saito, N., Abe, M. & Makino, S. (1998).The stability and convergence characteristics of the Delayed-X LMS algorithm in ANC systems, *Journal of Sound and Vibration,* 216(4), 637-648, pp. 637-648.

[10] Chen, G., Abe, M., & Sone, T. (1996). Effects of multiple secondary paths on convergence properties in active noise control systems with LMS algorithm, *Journal of Sound and Vibration*, 195, pp.217-228.

[11] Chen, G., Wang, H., Chen K., & Muto, K., (2008). The Influences of Path Characteristics on Multichannel Feedforword Active Noise Control System, *Journal of Sound and Vibration*, Vol.311, No.3, pp.729-736.
[12] Cowan, C. F. N., & Grant, P. M., (1985). *Adaptive filters*, Prentice-Hall Inc. Englewood Cliffs, New Jersey.
[13] Haykin, S. (1991). *Adaptive Filter Theory, 2nd ed*. Prenticehall Englewood Cliffs, Newyork.
[14] Widrow, B., McCool, J. M., Larimore, M. G. & Johnson. C. R., (1962) Stationary and nonstationary learning characteristics of the LMS adaptive filter, Proc. IEEE, 64 pp. 1151-1162.
[15] Chen, G., Abe, M., & Sone, T. (1996). Improvement of the convergence characteristics of the ANC system with the LMS algorithm by reducing the effect of secondary paths, *Journal of the Acoustical Society of Japan(E)*, Vol.17(6), pp.295-303.
[16] Kabel, P. (1983). The stability of adaptive minimum mean square error equalizers using delayed adjustment. *IEEE Transactions on Communications* COM-31, pp.430–432.
[17] Qureshi, S. K. H. & Newhall, E. E. (1973). An adaptive receiver for data transmission of time dispersive channels. *IEEE Transactions on Information Theory,* IT-19, pp.448–459.
[18] Elliott, .S. J., Baucher, C. C. & Nelson, P. A. (1991). The effects of modeling errors on the performance and stability of active noise control system. *Proceedings of the Conference on Recent Advances in Active Control of Sound and Vibration*, pp. 290–301.
[19] Saito, N. & Sone, T. (1996). Influence of modeling error on noise reduction performance of active noise control system using Filtered-x LMS algorithm, Vol. 17, pp.195–202. *Journal of the Acoustical Society of Japan (E)*.
[20] Kim, C. Abe, M. & Kido, K. (1983) Cancellation of signal picked up in a room by estimated signal. *Proceedings of Inter-noise 83,* pp.423–426.
[21] Saito, Y. Abe, M., Sone, T. & Kido, K. (1991). 3-D space active noise of sounds due to vibration sources. *Proceedings of the International Symposium on Active Control of Sound and Vibration*, pp. 315–320.
[22] Park, Y. & Kim, H. (1993). Delayed-x algorithm for a long duct system. *Proceedings of Inter-Noise 93*, pp. 767–770.
[23] Feintuch, P. L., Bershad, N. J., & Lo, A. K. (1993). A frequency domain model for "filtered" LMS algorithms-stability analysis, design, and elimination of the training mode, *IEEE Trans. Signal Process*, Vol. 41(3), pp. 1518-1531.
[24] Kurisu, K. (1996). Effect of the difference between error path C and its estimate C for active noise control using Filtered-x LMS algorithm. *Proceedings of Inter-Noise 96*, pp. 1041–1044.
[25] Chen, G., Wang, H., Chen K., & Muto, K.,(2005). A preprocessing method for multichannel feedforward active noise control, *Journal of Acoustical Science and Technology*, Vol. 26(3), pp.292-295.
[26] Wang, H., Chen, G. , Chen K., & Muto, K., (2006). Blind preprocessing method for multichannel feedforward active noise control. *Journal of Acoustical Science and Technology*, Vol. 27(5), pp.278-284.

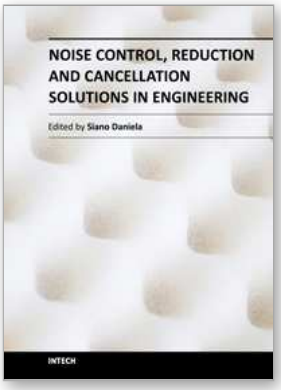

Noise Control, Reduction and Cancellation Solutions in Engineering

Edited by Dr Daniela Siano

ISBN 978-953-307-918-9
Hard cover, 298 pages
Publisher InTech
Published online 02, March, 2012
Published in print edition March, 2012

Noise has various effects on comfort, performance, and human health. For this reason, noise control plays an increasingly central role in the development of modern industrial and engineering applications. Nowadays, the noise control problem excites and attracts the attention of a great number of scientists in different disciplines. Indeed, noise control has a wide variety of applications in manufacturing, industrial operations, and consumer products. The main purpose of this book, organized in 13 chapters, is to present a comprehensive overview of recent advances in noise control and its applications in different research fields. The authors provide a range of practical applications of current and past noise control strategies in different real engineering problems. It is well addressed to researchers and engineers who have specific knowledge in acoustic problems. I would like to thank all the authors who accepted my invitation and agreed to share their work and experiences.

INTECH
open science | open minds

InTech Europe
University Campus STeP Ri
Slavka Krautzeka 83/A
51000 Rijeka, Croatia
Phone: +385 (51) 770 447
Fax: +385 (51) 686 166
www.intechopen.com

InTech China
Unit 405, Office Block, Hotel Equatorial Shanghai
No.65, Yan An Road (West), Shanghai, 200040, China
中国上海市延安西路65号上海国际贵都大饭店办公楼405单元
Phone: +86-21-62489820
Fax: +86-21-62489821